

Ordering and Recovery Processes in the Ni/Fe System near Ni₃Fe

C. F. VAROTTO, A. E. VIDOZ*

Instituto de Física "Dr. J. A. Balseiro" (Universidad de Cuyo) and Centro Atómico, San Carlos de Bariloche, Argentina

The ordering and recovery processes in 72/28 and 80/20 at. % Ni/Fe alloys have been investigated. A parameter related to the thermal scattering contribution of the electrical resistivity was used to follow the establishment of atomic order. It was found that the initial condition of the alloys – quenched or cold-worked – has little influence on the ordering kinetics at high temperatures. However, it greatly influences the recovery behaviour, as indicated by the residual resistivity measurements. Strain-ageing effects reported earlier are interpreted in the light of the present findings. Results are also discussed on the basis of existing theories for atomic ordering.

1. Introduction

The ordering behaviour of a metallic solid solution is modified by previous cold work. Concurrently, the recovery and recrystallisation processes are affected by the development of atomic order [1-5]. Interest in these complex phenomena has arisen during the investigation of the mechanical properties of Ni/Fe and Cu/Au alloys [2, 6-8], but so far no clear understanding of the interdependence of the processes has been achieved.

It is the purpose of this work to analyse the influence of cold work upon the atomic ordering of some Ni/Fe alloys in the proximity of Ni₃Fe. The ordering characteristics of these alloys have been the subject of several investigations [6, 9-13]. It is known that their critical order-disorder temperature, T_c , is 502°C for Ni₃Fe and slightly decreases with departure from stoichiometry, being approximately 480°C for the 80/20 at. % Ni/Fe alloy [2, 9, 12, 13]. The most favourable composition for order development is 73/27 at. % Ni/Fe with a maximum reported degree of order of 0.8 to 0.9 [6, 9, 13]. These Ni/Fe alloys are also characterised by very small domain size development [6, 9] as well as by low values of antiphase and stacking fault energies [14]. Although it is accepted that a small amount of order develops in the 80/20 at. % Ni/Fe alloy, the 78/22 at. % Ni/Fe alloy represents the limit of the Ni-rich

side of stoichiometry where appreciable ordering occurs [2, 9]. In the present work, the ordering behaviour of alloys with initial disordered conditions obtained by quenching from high temperatures or by cold-working has been investigated. The effect of ordering anneals has mainly been followed by means of electrical resistivity measurements, although in some particular cases X-ray diffraction and metallographic methods were used to determine the degree of recrystallisation.

The electrical resistivity results have been analysed by means of a procedure described in a previous publication [15] which allows the separation of the different contributions to the resistivity. It has been proved that for Ni/Fe alloys, below room temperature, the resistivity is given by:

$$\rho(A, W, T) = \rho_0(A, W) + \alpha(A) \cdot f(T) \quad (1)$$

where $\rho_0(A, W)$ is the residual resistivity, A and W are measures of atomic order and defect structure, respectively, T the temperature of measurements, and $\alpha(A) \cdot f(T)$ represents the thermal scattering contribution. Here $f(T)$ is a function of temperature only and $\alpha(A)$ is a parameter exclusively related to the state of atomic order and easy to determine experimentally. The results presented herein further serve to

*Now, Senior Member of the Research Laboratory, Lockheed Palo Alto Research Laboratory, 3251 Hanover Street, Palo Alto, 94304, California, USA

confirm the sole dependence of $\alpha(A)$ on the atomic order.

2. Experimental Procedure

The sources and analysis of materials, details of sample preparation and annealing treatments, as well as the techniques used for the measurement of electrical resistivity have already been described in previous publications [15, 16]. In most cases, duplicate specimens were used for each annealing run. Often, two runs were made for further checking on the reproducibility of results.

The short-term anneals (up to 60 min) were performed in a well-stirred salt bath with a temperature regulation of $\pm 0.5^\circ\text{C}$. Here the samples were wires (fabricated by swaging and drawing) of 0.6 mm in diameter and 100 mm length.

X-ray diffraction measurements were made with a Norelco diffractometer and cobalt radiation. For metallography, standard techniques for sample preparation and observation were used.

3. Experimental Results

The effect of isochronal and isothermal anneals on the electrical resistivity of disordered Ni/Fe alloy have been investigated. The isochronal anneals were performed first to determine the temperature zones where important structural changes take place. Then isothermal anneals were made at selected temperatures with the aim of characterising these modifications.

The following compositions were used: 66/34, 68/32, 71/29, 72/28, and 80/20 at.% Ni/Fe, respectively. However, only the results on the last two alloys, which are characteristic of the highest and lowest obtainable degrees of atomic order, will be presented here.

To establish the influence of cold work on the development of order as well as the effect of atomic order on the recovery and recrystallisation behaviour, two different initial disordered conditions were used: one was obtained by rapid quenching from well above the order/disorder critical temperature (T_c) and another by heavy cold-working after quenching. These conditions will be referred to as quenched and cold-worked, respectively.

3.1. Isochronal Anneals

The isochronal anneals were made with increments of temperature in steps of 25°C for several step-annealing times up to approximately T_c .

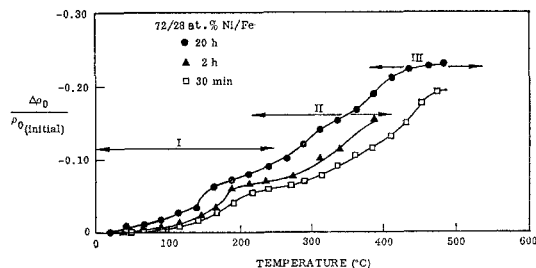


Figure 1 Relative changes of the residual resistivity ρ_0 upon isochronal anneals of a cold-worked 72/28 at.% Ni/Fe sample for three step-annealing times.

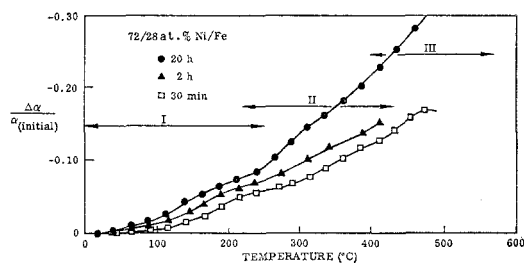


Figure 2 Relative changes of α upon isochronal anneals of a cold-worked 72/28 at.% Ni/Fe sample for three step-annealing times.

Figs. 1 and 2 show for the initially cold worked 72/28 alloy the relative variations of the residual resistivity ρ_0 and the parameter α (equation 1), respectively, versus the annealing temperature for three step-annealing times. The parameter α is here referred to as the standard cold-worked disordered condition [15]. Therefore, unless specially mentioned, $\alpha = 1$ for maximum achievable disorder. A similar representation for ρ_0 and α for the initially quenched alloy and a step-annealing time of 20 h is shown in fig. 3. There α and ρ_0 remain constants up to approximately 260°C . This temperature is similar to that

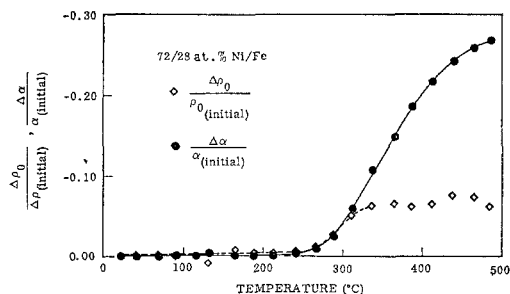


Figure 3 Relative changes of α and the residual resistivity ρ_0 upon an isochronal anneal for a quenched 72/28 at.% Ni/Fe sample. The step-annealing time is 20 h.

reported for vacancy migration in quenched pure Ni [17-19] and marks the onset of order development.

The effect of the initial sample condition of 72/28 alloy is more noticeable in fig. 4 where α is plotted versus temperature for both initially disordered conditions and a 20-h step-annealing time. For shorter step-annealing times, the second crossing of the curves takes place at higher temperatures (i.e., 350° for 2 h).

For the cold-worked and the quenched 80/20 alloy specimens, the effect of isochronal anneals with a 20-h step time on α and ρ_0 , is depicted by the results of figs. 5 and 6, respectively. Shorter step-annealing times show similar behaviour, with only minor temperature changes.

3.2. Isothermal Anneals

An examination of the isochronal results shows the presence of temperature regions in which different modes of resistivity variations indicate

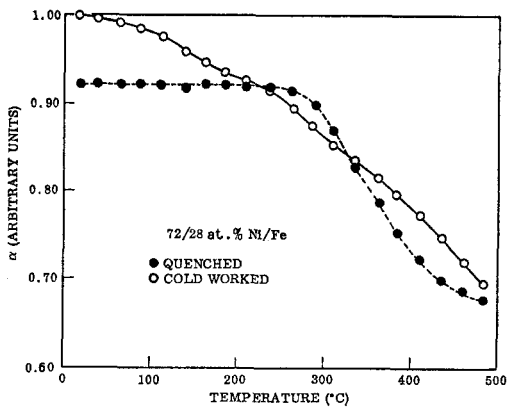


Figure 4 Changes of α upon an isochronal anneal for 72/28 at. % Ni/Fe samples in the quenched and cold-worked conditions. The step-annealing time is 20 h.

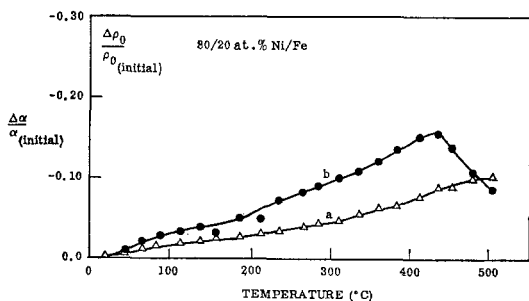


Figure 5 Relative changes of (a) residual resistivity ρ_0 and (b) parameter α upon an isochronal anneal of a cold-worked 80/20 at. % Ni/Fe sample. The step-annealing time is 20 h.

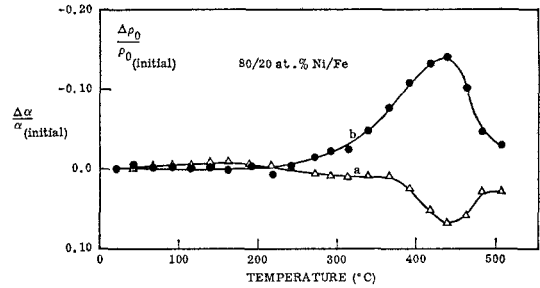


Figure 6 Relative changes of (a) residual resistivity ρ_0 and (b) parameter α upon an isochronal anneal of a quenched 80/20 at. % Ni/Fe sample. The step-annealing time is 20 h.

differences in the structural changes that take place. To obtain more information on the processes that occur during ordering-anneals, isothermal kinetics were examined at selected temperatures.

It has been reported that for these Ni/Fe alloys, the electrical resistivity, upon ordering, undergoes changes that have been classified into two distinct time classes [2]: short and long-term. Consequently, two types of isothermal anneals were made: one which involves maximum times of 1 h and another with anneals up to approximately 1000 h.

3.2.1. Initially Quenched 72/28 Alloy

Short- and long-term resistivity changes were measured at 401, 430, 470, and 482°C. The short-term measurements show poor reproducibility in the absolute values of α and ρ_0 , although there was qualitative agreement with the initial part of the long-term kinetics.

Fig. 7 shows the isothermal changes of α and ρ_0 for both quenched and initially cold-worked conditions at 458°C. For the as-quenched condition, while α decreases with time, the variation of ρ_0 show three distinct stages: an

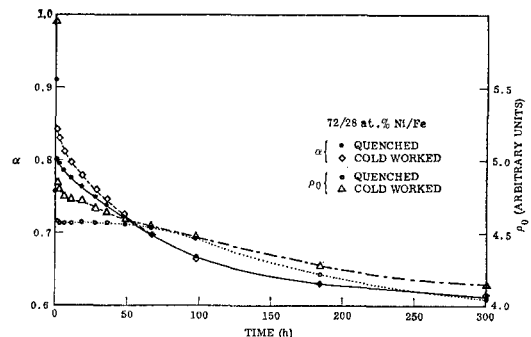


Figure 7 Changes of the residual resistivity ρ_0 and parameter α of a 72/28 at. % Ni/Fe samples upon isothermal anneals at 458°C.

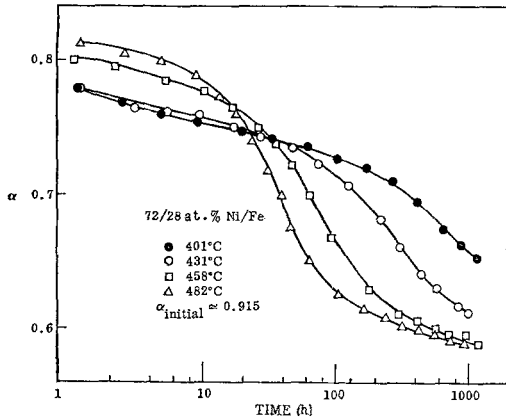


Figure 8 Changes of the parameter α of quenched 72/28 at.% Ni/Fe samples upon isothermal anneals at the indicated temperatures.

initial rapid decrease, a constant stage, and a final region where the residual resistivity decreases monotonically with time. This behaviour was typical of kinetics above 430°C, but for 401°C the second stage of ρ_0 was not observed. The extent of the second stage of ρ_0 and the annealing temperature do not seem to have a correlation pattern. In figs. 8 and 9 the values α and ρ_0 , respectively, are plotted versus the logarithm of annealing time. For long times, α shows a tendency to saturation which is not indicated by the measurements of ρ_0 . It should be pointed out here that although there is a kind of correlation between the general behaviour of α and ρ_0 , their time-dependence is undoubtedly different.

In fig. 10, α is plotted versus ρ_0 for several

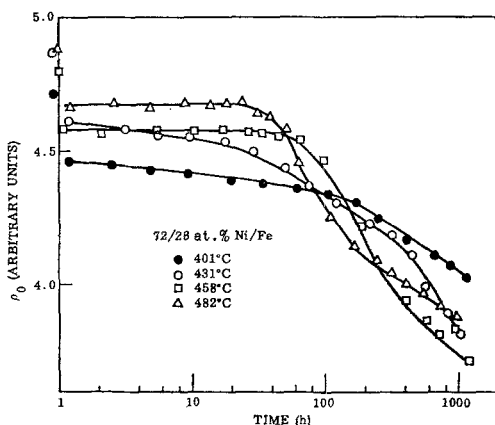


Figure 9 Changes of the residual resistivity ρ_0 of quenched 72/28 at.% Ni/Fe samples upon isothermal anneals at the indicated temperatures.

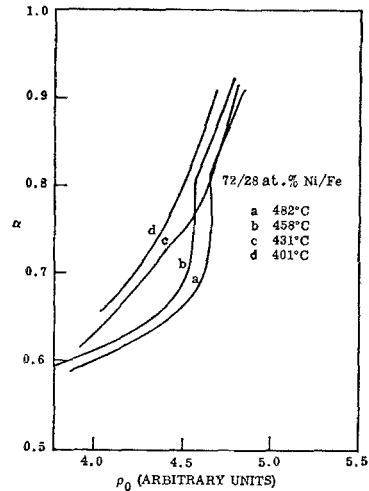


Figure 10 Parameter α versus the residual resistivity ρ_0 of quenched 72/28 at.% Ni/Fe samples upon isothermal anneals at indicated temperatures.

annealing temperatures. The differences in the initial values result from the difficulty of quenching into the sample the same initial condition. Here the three stages already described as well as the tendency of α toward saturation are more evident.

3.2.2. Initially Cold-Worked 72/28 Alloy

For this case, the isochronal results show the need for data over a wider temperature range. Consequently, long-term anneals were performed at 167, 241, 401, 413, 423, 431, 447, 458, 470 and 482°C. Only at five temperatures above 400°C were short-term measurements made, showing very good reproducibility of results.

The behaviour of α and ρ_0 upon isothermal annealing is depicted in fig. 7. Here also three regions of ρ_0 variation can be identified. The second stage, however, is not well defined and the changes in ρ_0 are smoother.

Figs. 11 and 12 plot, respectively, α and ρ_0 versus the logarithm of annealing time for several characteristic temperatures above 400°C. Fig. 13 plots α versus ρ_0 for these long-term kinetics, and in fig. 14 a similar representation is shown for the case of short-term, high-temperature, and long-term, low-temperature annealings. For the cold-worked case, the initial condition is very reproducible and consequently the initial values of α and ρ_0 were approximately the same for all samples. It is observed that there exists a unique correspondence between the α and ρ_0 values for both low- and high-temperature kinetics. This

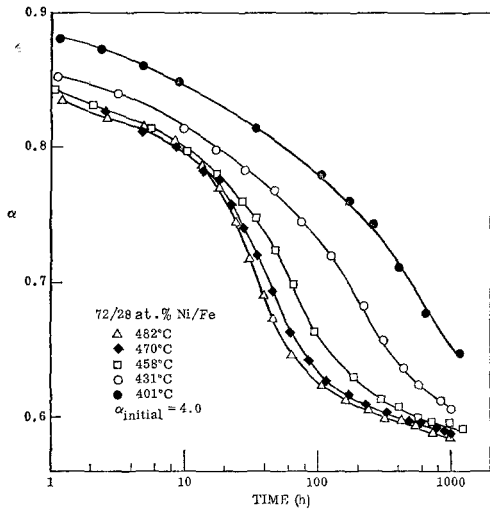


Figure 11 Changes of the parameter α of cold-worked 72/28 at. % Ni/Fe samples upon isothermal anneals at the indicated temperatures.

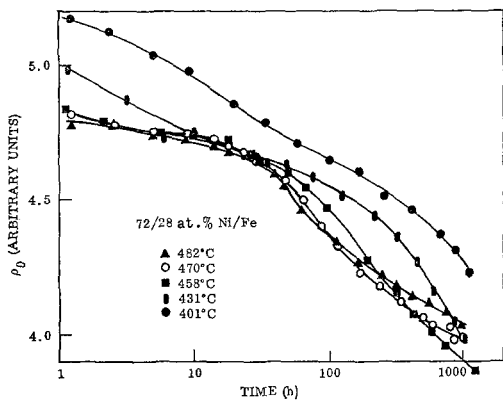


Figure 12 Changes of the residual resistivity ρ_0 of cold-worked 72/28 at. % Ni/Fe samples upon isothermal anneals at the indicated temperatures.

indicates that in both cases a similar ordering starts to develop. Unlike initially quenched material, here the curves of α versus time are in a simple correspondence with annealing temperature (fig. 11). This is indicated by the lack of crossings of the curves and the lower absolute values of α with increasing annealing temperature. The short-term kinetics show similar behaviour, with the exception of the 482°C case.

In figs. 15 and 16, the relative differences of α and ρ_0 between initially cold-worked and quenched material are plotted as a function of annealing time. It is noticeable that whereas α approaches the same final value for both initial

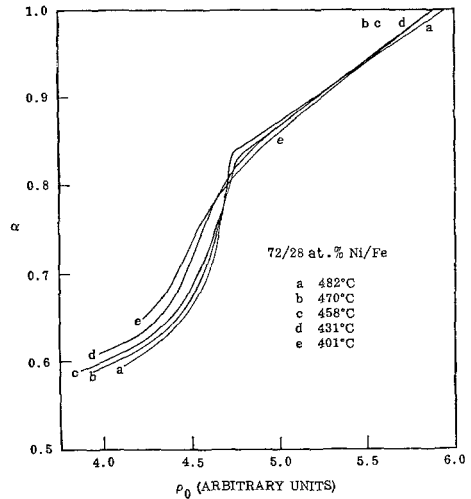


Figure 13 Parameter α versus the residual resistivity ρ_0 of cold-worked 72/28 at. % Ni/Fe samples upon isothermal anneals at indicated temperatures.

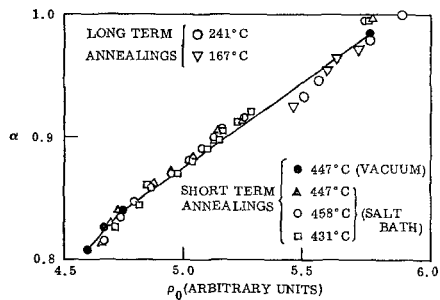


Figure 14 Parameter α versus the residual resistivity ρ_0 of cold-worked 72/28 at. % Ni/Fe samples upon several short- and long-term isothermal anneals as indicated.

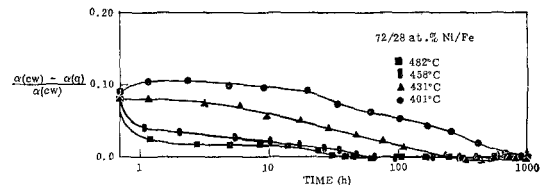


Figure 15 Relative differences of α between quenched and cold-worked 72/28 at. % Ni/Fe samples upon isothermal anneals at the indicated temperatures.

conditions of the alloy, ρ_0 shows final values about 4% greater for the cold-worked than for the as-quenched condition.

3.2.3. 80/20 at. % Ni/Fe Alloy

Long-term annealings were made at 401, 431, 458, 470, and 482°C. Figs. 17 and 18 plot the

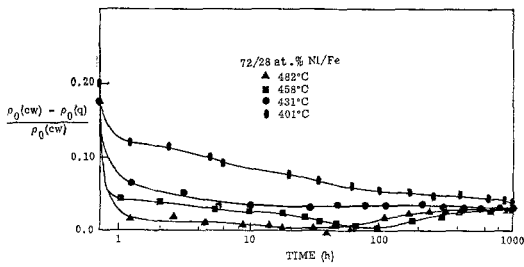


Figure 16 Relative differences of residual resistivity ρ_0 between quenched and cold-worked 72/28 at.% Ni/Fe samples, upon isothermal anneals at the indicated temperatures.

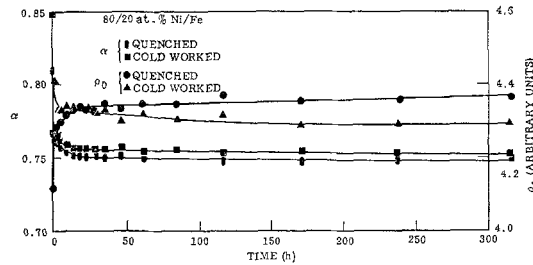


Figure 17 Changes of the residual resistivity ρ_0 and parameter α of quenched and cold-worked 80/20 at.% Ni/Fe samples upon isothermal anneals at 470°C.

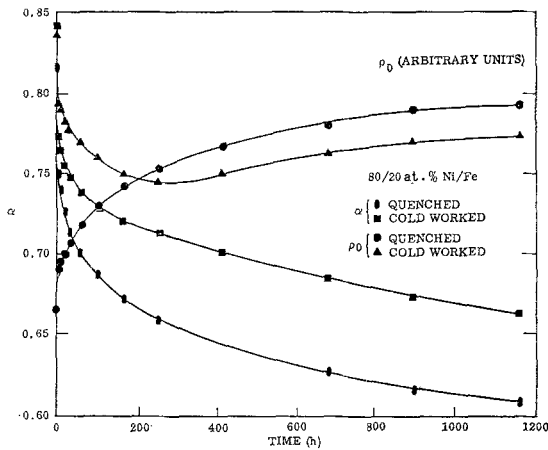


Figure 18 Changes of the residual resistivity ρ_0 and parameter α of quenched and cold-worked 80/20 at.% Ni/Fe samples upon isothermal anneals at 401°C.

values of α and ρ_0 versus the annealing time at 470° and 401°C, respectively, for both initially quenched and cold-worked conditions. Since this alloy develops a limited amount of order and concurrently shows only small changes in α and

ρ_0 , an enlarged scale has been used. Therefore, there is an apparent larger scatter of experimental results. For the as-quenched material, the parameter α decreases and the residual resistivity increases with annealing time. More complicated behaviour is observed for the cold-worked samples. While α for all cases decreases with time, ρ_0 after an initial decrease becomes constant for anneals at 470 and 480°C. However, for lower temperatures, instead of becoming constant, ρ_0 increases after the initial rapid decrease. This phenomenon, which was found to be very reproducible, did not take place in any other alloy so far investigated, including the extreme composition 66/34.

3.3. Recrystallisation Behaviour

Recrystallisation during annealing was investigated for the initially cold-worked 66/34, 68/32, 71/29, 72/28, and 80/20 alloys with both metallographic and X-ray diffraction techniques. The annealing temperatures used were 470, 482, 525, and 540°C. For the X-ray observations, the development of the (311) doublet was followed with Cok α radiation. Good agreement was found with most of the results previously reported [2]. However, the onset of recrystallisation was observed to occur at longer times and for the 72/28 alloy no indication of recrystallised nucleus formation was found at 482°C. This finding does not agree with the arrest of recrystallisation after 4 h of annealing at 480°C reported for a 73/27 alloy [2].

4. Interpretation of Experimental Results

In this section we shall discuss separately the results of the isochronal and isothermal anneals since they pose somewhat different problems.

4.1. Isochronal Anneals

The behaviour of the 72/28 alloy upon isochronal annealing may be divided into three temperature regions, as indicated in figs. 1 and 2. In the first one, the cold worked alloy shows a gradual decrease of both α and ρ_0 which may be attributed to ordering while vacancies migrate to combine with interstitials [17, 19]. This annihilation process changes the point defect concentration, and, since it implies mobility of vacancies, also modifies the first neighbour configuration and therefore affects both α and ρ_0 in a similar fashion. At approximately 140°C, an increase is observed in the rate of change of ρ_0 , identified in fig. 1 by a noticeable bump in the

curves. A similar, but less marked effect is also noticed for α (fig. 2). This change of behaviour occurs at a temperature where the vacancy recovery stage, stage IV, has been reported to start to develop during annealing of deformed pure Ni [17, 19]. Here vacancy mobility increases rapidly, resulting in both vacancy annihilation at sinks and further inducement of local order. Since α is only influenced by ordering [15] and ρ_0 by both order development and defect annihilation this process should affect the behaviour of ρ_0 more, in agreement with experimental findings. According to this explanation, the isochronal anneals of the quenched alloy show constant values of α and ρ_0 during this first stage (see fig. 3). This interpretation is further supported by the decrease in the size of the "bump" in fig. 1 for shorter step-annealing times. In the second temperature zone, the steady decrease of α (indicative of increase of order) with increasing temperature shown by the quenched material seems to indicate the occurrence of homogeneous ordering (see fig. 2). The behaviour of the cold-worked samples, however, appears still to be influenced by defect recovery. The difference between the rate of ordering of the cold-worked and the quenched specimens (fig. 4) may be due to the presence of the cold-worked structure in the former samples, affecting the mean free life of vacancies and therefore their efficiency for ordering.

The 80/20 alloy shows similar behaviour to the 72/28 alloy during the first and second temperature regions, although no increase in the rate of change of ρ_0 is observed near the end of the first zone (figs. 5 and 6). Since this alloy shows a peculiar increase in ρ_0 with annealing time (fig. 18), it is possible for it to compensate the effect of vacancy recovery. It is in the third temperature region where most of the isothermal anneals have been performed. Therefore, its discussion is included in the following section.

4.2. Isothermal Anneals

The parameter α , which has been shown to be dependent only on the atomic order [15], will be used here as the main tool for analysing the isothermal behaviour of the Ni/Fe alloys.

4.2.1. 72/28 Ni/Fe Alloy Initially Quenched

The rapid establishment of (short range) order at the beginning of the isothermal anneals, as indicated by the decrease of α in fig. 7, is undoubtedly related to the migration of excess

quenched-in vacancies. In this stage, the efficacy of vacancies in inducing order has to be related to the excess concentration of vacancies, their mean free path to annihilation, and the driving force for ordering which will be dependent on the equilibrium and actual degree of order of the system. Since the concentration of both vacancies and sinks is established by the quenching procedure, the rate of ordering, and the degree of order produced by the migration of quenched-in vacancies, has to be controlled by the magnitude of the driving force. This force, being greater the lower the temperature, results in a greater degree of (short range) order, at short annealing times, for the lower annealing temperatures. This effect is clearly shown in fig. 8 and is in agreement with the proposed ordering behaviour for the A_3B type of structures [22]. In these alloys, Iida [10, 11] has observed SRO to develop faster, the nearer the annealing temperature is to the order-disorder transition. However, since his stored energy measurements were made after annealing at slightly above T_c , the initial ordering stage described above was probably not observed.

After the rapid initial ordering, the behaviour of the isothermal kinetics follows a similar trend to the stored energy [10, 11] at comparable temperatures. In fig. 19 the time-variation of $d\alpha/dt$ is plotted versus annealing time. Also represented is the variation of the stored energy dv/dt at 490°C [10, 11]. The agreement between the present results and the measurements of Iida further stresses the unique relationship between α and atomic order. Ordering is now probably occurring by a vacancy interchange mechanism controlled by the mobility of vacancies in

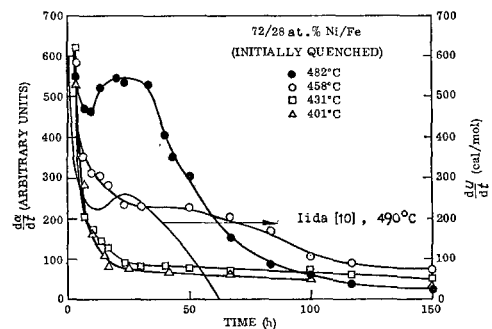


Figure 19 Time-derivative of α ($d\alpha/dt$) versus annealing time upon isothermal anneals of quenched 72/28 at.% Ni/Fe samples. The time derivative of the internal energy dv/dt of Ni_3Fe at 490°C as measured by Iida [10] are also indicated.

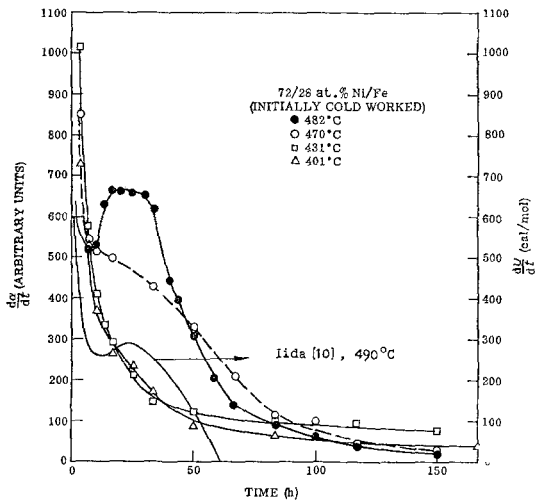


Figure 20 Time-derivative of α ($d\alpha/dt$) versus annealing time upon isothermal anneals of cold-worked 72/28 at. % Ni/Fe samples. The time-derivative of the internal energy dU/dt of Ni₃Fe at 490°C as measured by Iida [10] are also indicated.

thermal equilibrium. Therefore, its rate will be greater, the higher the annealing temperature, in agreement with the results of figs. 8 and 19. It has been recognised that in Ni₃Fe type alloys, LRO follows after prolonged annealing times [2, 6, 9-11]. The establishment of this order condition may depend strongly on the annealing temperature.

For the case of high temperatures (near T_c) further ordering may occur by nucleation and growth with an initial distribution of coarse nuclei (with low degree of LRO) in a SR ordered matrix. A similar situation to that proposed here has been observed for Cu₃Au in which ordered precipitates co-exist with a disordered matrix [21].

At lower temperatures, since the initially developed degree of SRO is greater, the probability for nucleation of LRO becomes higher than before and consequently a finer LRO nucleation covering most of the material may be expected. Therefore, homogeneous ordering should predominate on further annealing. The proposed ordering mechanisms seem to be consistent with the behaviour of the residual resistivity ρ_0 which upon annealing presents three characteristic stages (see fig. 7). The first stage at the beginning of annealing, shows a rapid decrease of ρ_0 accompanying the decrease of α . This reflects the annihilation of defects as well as the local order development. The slightly greater

decrease in ρ_0 for the lower temperatures agrees with the higher order observed for this case. The second stage, showing a constant ρ_0 for high temperatures, is altogether absent in the low-temperature kinetics. This effect is better shown in fig. 10 where α is plotted versus ρ_0 for several annealing temperatures. Here it is observed that for equal degree of order (and consequently equal value of ρ_0) is the smaller, the lower the annealing temperature. It is possible that some additional scattering source is present and gives rise to the observed dependence on the annealing temperatures. Finally, the third stage is assumed to be due to homogeneous ordering near or at coalescence.

4.2.2. 72/28 at. % Ni/Fe Alloy Initially Cold-Worked

For the cold-worked alloys, a rapid initial decrease of both α and ρ_0 upon annealing is also observed, as shown in figs. 11 and 12 (note the high initial value of α , which may be adequately described by a similar vacancy migration-inducing ordering mechanism. Cold-work, however, produces a condition necessarily more complicated than in quenched specimens, since not only vacancies, but also interstitials, dislocations, and other complex structural defects are generated and a more highly disordered state is achieved. This is indicated by the initial values of α and ρ_0 (compare figs. 8, 9, 11 and 12). The high dislocation density created by cold-work influences also the migration of vacancies, since the number of sinks available for vacancy annihilation increases. Upon annealing, most of the excess vacancies recombine with interstitials, a process that requires only short-range motion. The remaining vacancies migrate towards sinks located at shorter distances than in the case of initially quenched material. Therefore, although the number of excess vacancies in the cold-worked is much greater than in the quenched case, their mean free path toward annihilation is also smaller, reducing accordingly their efficacy for ordering. This explanation accounts for the similarity between the magnitude of the initial decrease of α (or increase in degree of order) shown by the samples in both initial conditions.

It is established by these results without any doubt that upon annealing atomic order develops very rapidly in the Ni/Fe alloys. The fast formation of order should account for the changes in mechanical properties as proposed by Vidoz *et al* [2]. The pronounced increase in strength upon

short-term annealing observed for the cold-worked samples, compared with the slight increase of strength in the quenched specimens [2], is now readily attributed to the initial degree of order of the specimens. For the latter case, a substantial degree of local order is initially present while for the former condition the material is nearly disordered. Therefore, it would be expected that an increase in the degree of order upon annealing will introduce a much greater additional difficulty for dislocation motion in the cold-worked alloy, where no order was initially present, than in the quenched material in which hardening due to local order was already active.

The degree of order established in the cold-worked samples by this initial rapid process has a different annealing temperature-dependence to that of the quenched material. The higher the temperature, the greater the degree of order and consequently the quicker rate of ordering. This effect may be related to the concurrent recovery of the cold-worked dislocation structure. The effect, which is more important at higher temperatures, results in increasing the vacancy mean free path by decreasing the number of available sinks. Therefore, the efficacy of vacancies for ordering becomes greater at the higher annealing temperature, overcoming the effect of the smaller driving force and giving place to the temperature-dependence of α shown in fig. 11. This process accounts also for the initial changes of ρ_0 (see fig. 12) the greater the changes the higher the annealing temperatures. An activation energy was calculated for the process occurring at short annealing times, disregarding the data for the highest annealing temperatures where some anomalies take place, due perhaps to recovery or different driving forces. A value for the activation energy of 1.47 eV was obtained, which is very similar to the value obtained for vacancy migration in pure Ni [17, 19, 23]. This activation energy was computed assuming an Arrhenius temperature-dependence for the times at which, for the several kinetics, equal values of α were achieved [22]. This further indicates that at this initial stage ordering takes place by migration of excess vacancies. Interesting to note are the results shown in fig. 14 where α is plotted versus ρ_0 for the cases already discussed and also for two very low annealing temperatures (167 and 241°C) corresponding to the second stage of variations in the isochronal anneals. The agreement between the values is again an indication

that ordering at this first stage is generated, at all annealing temperatures, by the same process. After this initial period, the rate of ordering of the cold-worked alloys is very similar to the quenched case (figs. 19 and 20); however, the presence of the cold-worked structure continues to influence the ordering behaviour of Ni/Fe, assuming the nucleation of antiphase domains is more copious than for quenched samples and domain growth is limited by the changes of the dislocation configuration. Therefore, at all annealing temperatures one may suppose that homogeneous ordering of the domains is the rate-controlling process. Domain growth which depends on dislocation recovery is here much lower than for quenched samples [2].

The results of fig. 7 show that the ordering behaviour of the cold-worked samples does not differ much from that of the quenched specimens. A similar second stage of ρ_0 is noticed. Here the residual resistivity decreases slightly instead of being constant, which further indicates the occurrence of recovery. For an equal degree of order (equal α) also, ρ_0 increases with rising annealing temperatures, supporting the hypothesis of an additional scattering source. At long annealing times, there is a constant difference between the values of the residual resistivity of the cold-worked and quenched specimens. This may be attributed to the presence of numerous dislocations in the cold-worked samples, since in this annealing condition recrystallisation does not take place. Assuming a contribution to the resistivity due to dislocations given by $\Delta\rho = k \cdot d$ where d is the dislocation density and K a constant, and using for these alloys a value for $K = 9.4 \times 10^{-13} \mu\Omega \text{ cm}^3$ given for pure Ni [24, 25] a value of $d = 1.9 \times 10^{11} \text{ cm}^{-2}$ was calculated from the constant measured difference of resistivities. This value is in good agreement with the value of 10^{11} cm^{-2} reported for 70% cold-worked Ni [26]. Finally, although significant recovery occurs in this alloy, there was not a single piece of evidence for the occurrence of recrystallisation, in contradiction with previous results [2].

From the above discussion it can be concluded that defect recovery influences the ordering behaviour during the first and second stages of the kinetics. However, this influence does not imply much difference in the ordering mechanism, as is inferred from the similarity between the ordering rates for both cold-worked and quenched samples. Cold-work evidently destroys

the order acquired by the alloys during quenching. However, this degree of order is rapidly recovered by the material upon annealing.

4.2.3. 80/20 at. % Ni/Fe Alloy

Upon annealing, the quenched and cold-worked 80/20 samples show rapid changes of α and ρ_0 which are attributed to the mechanisms discussed before: order induced by vacancy migration and recovery of defects. Although α decreases with annealing time, indicating the establishment of atomic order, ρ_0 shows the following behaviour which requires further discussion: (a) Increases with annealing time for the quenched specimens (figs. 17 and 18).

(b) Decreases initially, achieves a minimum and increases on further annealing for the cold-worked samples (figs. 17 and 18).

Let us discuss these results in order.

(a) Several interpretations may be advanced to explain the increase of ρ_0 upon annealing. One of them [27] proposes that the formation of SRO may lead to resistivity increase. Another uses an idea based on the modification of the Fermi surface intercepting new boundaries created by order development [28]. However, since this alloy develops small amounts of order [2] and none of the other compositions investigated show the effect, it seems improbable for the above hypothesis to explain the observed increase of ρ_0 . Another possibility may be considered to explain the phenomenon. The development of order may occur in this alloy by the formation of order nuclei with quasi-stoichiometric composition. Around the nuclei, zones of high Ni concentration have to exist which make further growth of the small ordered regions difficult. The combination of order and composition gradient may give rise to the resistivity increase. Segregation of Ni should be reduced at higher temperatures where the degree of order is smaller (fig. 17), allowing the formation of larger domains, in agreement with the smaller values of ρ_0 at higher temperatures.

(b) For the initially cold-worked specimens, the inversion of ρ_0 results from the competition of local order development and recovery of the cold-worked structure. It is observed that the ρ_0 inversion point occurs at all temperatures at approximately the same value of α and ρ_0 . Therefore, it is displaced to longer times the lower the annealing temperature. Assuming that the inversion time follows an Arrhenius type of dependence with temperature, an activation

energy of 2.1 eV was calculated. This value is similar to that for self-diffusion of Ni in the 80/20 alloy [29], supporting the hypothesis that the process is controlled by Ni segregation. After prolonged annealing at 470 and 482°C, full recrystallisation of the cold-worked material occurs. This accounts for the finding that this material has lower ρ_0 than the quenched samples and an equal degree of order for long annealing times.

Acknowledgements

The authors acknowledge the assistance of Mr D. Vasallo and Mr R. Runge and the stimulating discussions with Dr J. Kittl. This work was partially supported by the US Army Research Office.

References

1. G. GUARINI, *Nuovo Cim.* **44B** (1966) 129.
2. A. E. VIDOZ, D. P. LAZAREVIĆ, and R. W. CAHN, *Acta Met.* **11** (1963) 17.
3. V. S. ARUNACHALAM and R. W. CAHN, *J. Mater. Sci.* **2** (1967) 160.
4. C. L. COREY and D. I. POTTER, *J. Appl. Phys.* **38** (1967) 3894.
5. B. ROESSLER, D. T. NOVICK, and M. B. BEVER, *Trans. AIME* **227** (1963) 985.
6. R. G. DAVIES and N. S. STOLOFS, *Acta Metallurgica* **11** (1963) 1347.
7. T. SUZUKI and M. YAMAMOTO, *J. Phys. Soc. Japan* **14** (4) (1959) 463.
8. C. A. PAMPILLO, Doctoral Thesis, Instituto Balseiro, Univ. de Cuyo, Argentina (1967).
9. R. J. WAKELIN and E. L. YATES, *Proc. Phys. Soc.* **B66** (1953) 221.
10. S. IIDA, *J. Phys. Soc. Japan* **7** (1952) 373.
11. *Idem, ibid* **9** (1954) 346.
12. E. JOSSO, *CR Acad. Sci., Paris* **230** (1950) 1467.
13. I. M. PÜZEL, *Phys. of Metals and Metallography* **11** (5) (1961) 44
14. M. FAYARD and F. BEHOT, *CR Acad. Sci., Paris* **256** (1963) 3668.
15. C. F. VAROTTO and A. E. VIDOZ, *Phys. Status Solidi (a)*, **3** (1970) 697.
16. *Idem, ibid* **18** K49 (1966).
17. D. SCHUMACHER, W. SCHÜLE, and A. SEEGER, *Z. Naturf.* **17a** (1962) 228.
18. F. BELL, *Acta Metallurgica* **13** (1965) 363.
19. H. KRESSEL, W. SHORT, and N. BROWN, *ibid* **15** (1967) 525.
20. G. J. DINIES, *ibid* **3** (1955) 549.
21. A. COMANZI and G. SCHIANCHI, *J. Mater. Sci.* **5** (1970) 271.
22. A. C. DAMASK and G. J. DIENES, *Points Defects in Metals* (Gordon and Breach, New York, 1964).
23. P. SIMON and R. SIZMANN, *Z. Naturf.* **17a** (1962) 596
24. J. FRIEDEL, *Dislocations* (Addison-Wesley, 1964).

25. L. M. CLAREBROUGH, M. E. HARGREAVES, and M. H. LORETTO, *Phil. Mag.* **6** (1961) 807.
26. L. M. CLAREBROUGH, M. E. HARGREAVES, M. H. LORETTO, and G. W. WEST, *Acta Metallurgica* **8** (1960) 797.
27. M. T. BEAL, *Rapport CEA (France)* (1963) 2304.
28. A. MARCHAND, Doctoral Thesis, Grenoble, France (1966).
29. E. WALSOE DE RECA and C. PAMPILLO, *Acta Metallurgica* **15** (1967) 1263.

Received 24 November and accepted 13 January 1971.